

Multiatom interactions in the fcc Ising binary alloy: Low-temperature behavior and Monte Carlo simulations

Daniel F. Styer,* Mohan K. Phani,[†] and Joel L. Lebowitz

Department of Mathematics and Department of Physics, Rutgers University, New Brunswick, New Jersey 08903

(Received 23 September 1985)

We investigate an Ising model of an ordering binary alloy on the face-centered-cubic lattice, such as Cu-Au. This model contains multiatom interactions on the triangles and tetrahedra of the lattice as well as the usual repulsions on the nearest-neighbor bonds. We examine the model's ground states and its low-temperature equilibrium states: There are an infinite number of the former but only a few of the latter. We also study its phase diagram using Monte Carlo simulations, which confirm the broad conclusions of previous cluster-variation-method calculations, particularly near stoichiometry. Even small triangular interactions can introduce dramatic asymmetry into the phase diagram, making it similar to those observed in real alloys.

I. INTRODUCTION

The use of nearest-neighbor Ising models to approximate binary alloys has had a long and distinguished history.¹⁻⁹ It is, however, clear that such models, which contain only two parameters (the coupling constant and the magnetic field), cannot hope to explain the tremendous variety of alloy phase diagrams found in nature. One way to make the model both more realistic and more general is by adding second- or even further-neighbor interactions.⁶⁻¹⁷ However, any Ising model with pair interactions alone, regardless of their range or complexity, is symmetric between the two constituent species and hence the resulting phase diagram must be symmetric about 50% composition. (Although this symmetry does not arise if the pair interaction strengths depend upon composition, such interactions are in fact not pair interactions at all, because the "pair" energy depends upon all the sites used to find the average composition.) Realistic, asymmetric phase diagrams can be obtained only from models with multiatom interactions, and this paper investigates the phase diagram of one such model.

We choose to study an Ising model for face-centered-cubic alloys which has four parameters, corresponding to one-, two-, three-, and four-body interactions. In each case the n -body interaction extends over the smallest n -site unit of the fcc lattice, e.g., over nearest-neighbor bonds, and over the smallest triangles and tetrahedra of the lattice. While this model, which was suggested by van Baal² and studied by Kikuchi and collaborators,¹⁸⁻²² is still only a caricature of real fcc alloys such as copper-gold, we shall see that it nevertheless captures the asymmetry of the real systems.

The nearest-neighbor Ising model on the fcc lattice has been investigated using several techniques, most prominently the cluster-variation method²⁻⁵ (CVM) and Monte Carlo simulation⁶⁻⁹ (for a review see Ref. 5). These investigations support a picture with five distinct types of zero-temperature ground states which become, at finite temperatures, four distinct phases separated by first-order

phase boundaries. Here we ask how this symmetric phase diagram is altered by the addition of small multiatom interactions, and find that it remains topologically unaltered but that even very small three-body interactions can induce dramatic asymmetry. Previous work on this model¹⁹ (performed using the tetrahedron approximation of the CVM) found that a reasonable likeness of the experimental copper-gold phase diagram could be obtained easily by adjusting only two parameters in the model Hamiltonian. The surprise of such good agreement from so simple a model raises the possibility that the CVM phase diagram is a product more of the approximation used to produce it than of the true phase diagram of the model Hamiltonian. To test this possibility we studied the same system using high-accuracy Monte Carlo simulations, and these simulations have verified the broad outlines of the CVM results. Specifically, the transition temperatures predicted by the CVM are accurate to within 5% or 10% near stoichiometry, but the situation away from stoichiometry is less clear.

We begin this paper with a detailed specification of the model in both binary-alloy and Ising-spin language (Sec. II). We use geometrical arguments to uncover the model's highly degenerate ground states (Sec. III), and Pirogov-Sinai theory to investigate the low-temperature states as perturbations of these ground states (Sec. IV). In Sec. V (which is independent of Secs. III and IV) we extend our treatment to arbitrary temperatures (but at particular interaction strengths) using Monte Carlo simulation. This section emphasizes the transitions and phase diagram of the model. Although in this paper we focus on applications of the multiatom Ising model to alloy systems, it is also applicable to physical problems as diverse as the phase diagrams of metal hydrides²³ and classical fluids,²⁴ the magnetism of solid ³He,²⁵ and even lattice gauge theories.^{26,27}

II. THE MODEL

A face-centered-cubic lattice of N sites (and with periodic boundary conditions) possesses $6N$ nearest-

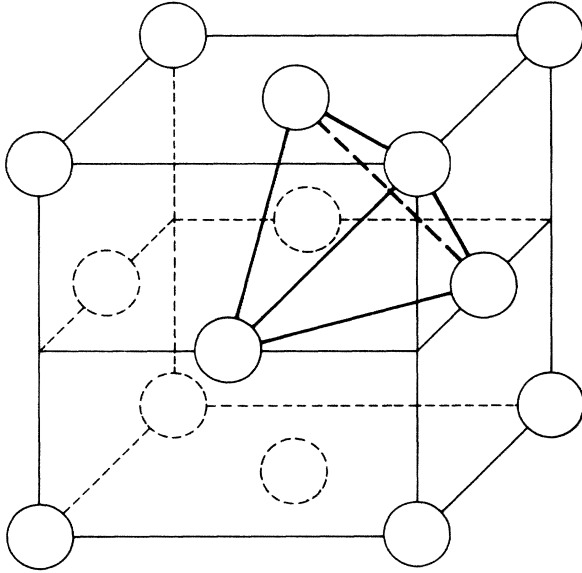


FIG. 1. The conventional unit cell of the face-centered-cubic lattice. The thin lines are next-nearest-neighbor bonds, the thick lines are nearest-neighbor bonds. The four nearest-neighbor bonds shown make up four triangles and one tetrahedron. Although the conventional unit cell holds eight such tetrahedra, one in each corner, only one is shown for clarity.

neighbor bonds. These bonds form $8N$ equilateral triangles and $2N$ tetrahedra. These are illustrated in Fig. 1, and will subsequently be referred to simply as "bonds," "triangles," and "tetrahedra," without the nearest-neighbor qualifier. We consider a spin- $\frac{1}{2}$ Ising model on this lattice, with spin variable $s_i = \pm 1$ at each lattice site i , and with interaction Hamiltonian

$$\mathcal{H} = J_2 \sum s_i s_j + J_3 \sum s_i s_j s_k + J_4 \sum s_i s_j s_k s_l - mH \sum s_i + J_0 N. \quad (1)$$

The four sums run over all bonds, all triangles, all tetrahedra, and all sites in the lattice, respectively. We will restrict our attention to the model with antiferromagnetic bond interactions, i.e., with $J_2 > 0$. (Note that only the three-spin interaction introduces asymmetry with respect to field in the resulting phase diagram, because clusters of even number must preserve the symmetry.) While there are five coupling strengths in this Hamiltonian, investiga-

tors in magnetics conventionally set $J_0 = 0$ to fix the energy zero.

It is frequently convenient to write the Hamiltonian as a sum over tetrahedra alone. Each tetrahedron is in one of only five distinguished configurations: all spins up, one down, two down, three down, and all down. We refer to these configurations by the number of down spins they contain: e.g., a type-3 tetrahedron contains three down spins and one up spin. Because each bond is shared by two tetrahedra, and each site by eight tetrahedra, the energy contribution of a type- n tetrahedron is ϵ_n , where

$$\begin{aligned} \epsilon_0 &= 3J_2 + 4J_3 + J_4 - \frac{1}{2}mH + \frac{1}{2}J_0, \\ \epsilon_1 &= -2J_3 - J_4 - \frac{1}{4}mH + \frac{1}{2}J_0, \\ \epsilon_2 &= -J_2 + J_4 + \frac{1}{2}J_0, \\ \epsilon_3 &= 2J_3 - J_4 + \frac{1}{4}mH + \frac{1}{2}J_0, \\ \epsilon_4 &= 3J_2 - 4J_3 + J_4 + \frac{1}{2}mH + \frac{1}{2}J_0. \end{aligned} \quad (2)$$

If N_n represents the number of type- n tetrahedra, the Hamiltonian may be rewritten as

$$\mathcal{H} = \epsilon_0 N_0 + \epsilon_1 N_1 + \epsilon_2 N_2 + \epsilon_3 N_3 + \epsilon_4 N_4. \quad (3)$$

(Recall that the sum $N_0 + N_1 + N_2 + N_3 + N_4$ is $2N$, not N .) In this language, a convenient energy zero is fixed by taking, say, $\epsilon_2 = 0$.

Workers in binary alloys use yet a third form for the Hamiltonian. This form starts by taking the total energy of an AB alloy to be

$$\mathcal{H}_{AB} = -\frac{3}{2}v(1+\alpha)N_1 - 2vN_2 - \frac{3}{2}v(1+\beta)N_3, \quad (4)$$

where N_n is now the number of tetrahedra whose four sites hold exactly n B atoms. [The B atoms in alloy language correspond, by common convention, to down spins in Ising language. Also, our energy parameter v is equal to Kikuchi and de Fontaine's $-\epsilon_{12}$ (Ref. 18) and to Cahn and Kikuchi's $-w$ (Ref. 20), so v is positive in this work: see Ref. 8. Because the canonical Ising model corresponds to the grand canonical binary alloy, the \mathcal{H} in (1) corresponds to

$$\mathcal{H}_{AB} - \mu_A N_A - \mu_B N_B, \quad (5)$$

where N_A is the number of A atoms in the lattice and N_B the number of B atoms. In alloy language, the energy zero is most conveniently fixed by taking

$$-\mu_A = \mu_B \equiv \mu, \quad (6)$$

in which case (5) is

$$\frac{\mu}{2} N_0 + \left[-\frac{3}{2}v(1+\alpha) + \frac{\mu}{4} \right] N_1 - 2vN_2 + \left[-\frac{3}{2}v(1+\beta) - \frac{\mu}{4} \right] N_3 - \frac{\mu}{2} N_4. \quad (7)$$

The correspondence between the alloy and Ising systems is achieved when

$$\begin{aligned} v &= 2J_2, \\ \alpha &= (4J_3 + 2J_3)/(3J_2), \end{aligned}$$

$$\beta = (-4J_3 + 2J_4)/(3J_2), \quad (8a)$$

$$\mu = 8J_3 - mH,$$

or, in other words, when

$$\begin{aligned}
 J_2 &= \frac{1}{2}v, \\
 J_3 &= \frac{3}{16}v(\alpha - \beta), \\
 J_4 &= \frac{3}{8}v(\alpha + \beta), \\
 mH &= \frac{3}{2}v(\alpha - \beta) - \mu, \\
 J_0 &= -\frac{3}{4}v(4 + \alpha + \beta).
 \end{aligned}
 \tag{8b}$$

Two features of this correspondence are noteworthy. First, pure pair interactions correspond to $\alpha = \beta = 0$. Second, magnetic field and chemical potential difference are not proportional, as they are in the pair interaction case, because there is an offset proportional to J_3 .

III. GROUND STATES

The ground states of this model, or of various simplifications of it, have been investigated previously,^{20,28-32} but not, we believe, in the simple manner used here. The ground states are in fact found effortlessly from the Hamiltonian in form (3) by noting that when, for example, ϵ_1 is the smallest of the five parameters ϵ_n , then any configuration in which every tetrahedron has exactly one down spin is a ground state. We must of course also convince ourselves that such configurations exist, because a local prescription such as "every tetrahedron has exactly one down spin" can be inconsistent. (For example, the prescription "every nearest-neighbor bond connects an up spin and a down spin" is inconsistent.) Because the prescriptions are in fact consistent there are five kinds of ground states, which we name after their constituent tetrahedra: the ground state formed entirely of type- n tetrahedra (that is, tetrahedra of n down spins) is called a type- n ground state. This classification breaks the multidimensional parameter space into regions according to the type of tetrahedron which is most stable in that region. This "zero-temperature phase diagram" also has surfaces of lower dimension in which two or more of the ϵ_n parameters are smallest.

In the next section we will use Pirogov-Sinai theory to "continue" this zero-temperature phase diagram into the low-temperature regime. In this section, however, we describe and analyze the ground states. We will first prove the consistency of the five ground-state prescriptions by demonstrating spin configurations in which they are trivially satisfied. (For three of the prescriptions we actually demonstrate an infinite number of such configurations.) We then prove that these configurations are the only ground states by describing the procedure used to construct them: casual readers will want to skip these detailed arguments. In addition, Fig. 2 converts the zero-temperature phase diagram in terms of the variables ϵ_n into a phase diagram in terms of the more familiar variables α , β , and μ .

It is easy to find the single configuration consisting entirely of type-0 tetrahedra: it is the one in which all spins point up. Similarly, in the type-4 ground state all spins point down. The three remaining kinds of ground states are more complex: they are described in terms of (100) planes (for example, the planes defined by the bottom five sites, the middle four sites, or the top five sites in Fig. 1).

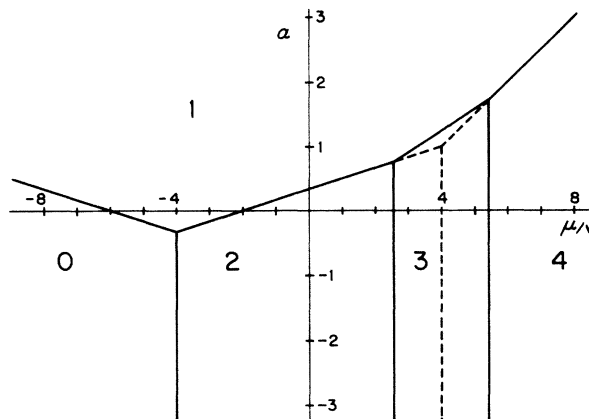


FIG. 2. Ground-state phase diagram with $\beta = -0.1$. The diagram maintains this same general form for $-\frac{1}{3} < \beta < 1$. In this regime the 2-3 phase boundary is $\mu/v = 2 - 6\beta$, and for all $\beta > -\frac{1}{3}$ the 3-4 phase boundary is $\mu/v = 6 + 6\beta$ and the 1-3 phase boundary is $\mu/v = 3\alpha - 3\beta$. (For all $\beta > -\frac{1}{3}$ the 1-3 phase boundary is simply a straight line connecting the tops of the right- and left-hand boundaries of the type-3 phase.) The remaining phase boundaries are β independent and their equations can be read off the graph. If β decreases from -0.1 the type-3 phase region shrinks until, at $\beta = -\frac{1}{3}$, it vanishes by collapsing onto the dashed line. Further decrease in β has no effect on the phase diagram. If β increases from -0.1 the type-3 phase expands into the type-2 and type-4 phase regions, until at $\beta = 1$ the type-2 phase vanishes. For $\beta > 1$ the 0-3 phase boundary is $\mu/v = -2 - 2\beta$, so further increase in β results in further expansion of the type-3 phase.

Each such plane (or "layer") supports a two-dimensional square lattice. We call a layer "spin up" if all the spins in its square lattice point up, "spin down" if they all point down, and "checkered" if they point alternately up and down. (In other words, every nearest-neighbor bond within a checkered layer connects spins of opposite sign.) Note that while the up and down configurations are unique, there are two different ways to checker a layer, depending upon which of the two sublattices holds the up spins. The type-1 ground state consists of alternating spin-up and checkered layers. Because the checkered layers can be either of two varieties, there is a ground-state degeneracy of order $3(2^{l/2})$, where l is the number of layers in the lattice. (A cube with L unit cells on an edge has $l = 2L$ layers and $N = 4L^3$ sites.) The prefactor three corresponds to the three sets of (100)-like planes [i.e., (100) planes, (010) planes, and (001) planes]. Similarly, the type-3 ground state consists of alternating spin-down and checkered planes. Finally, the type-2 ground state consists entirely of checkered layers, and has degeneracy of order $3(2^l)$.

On the phase boundaries of the zero-temperature phase diagram two or more of the ϵ_n are smallest. Here the ground states are even more degenerate and correspondingly more difficult to describe globally. In general, one expects that such states will violate the third law of ther-

modynamics and possess finite entropy per site at zero temperature (see, for example, Ref. 33). Such ground states are called "superdegenerate."¹¹

We now show how to construct the ground states described above, beginning with the type-2 ground state. The construction proceeds in two steps: first, we find which conventional unit-cell configurations can be formed from type-2 tetrahedra, and then we show that such unit cells can be pieced together only in the manner given. The reader may readily verify for himself that there are only three conventional unit cells in which all eight constituent tetrahedra are of type 2. Two of these cells, the so-called D and S cells, are shown in Fig. 3. The third, or S' , cell is simply the S cell with all spins reversed. (When all the spins of a D cell are reversed, one obtains another D cell, upside down relative to the one in Fig. 3.) Note that the D cell is the only one in which next-nearest neighbors are of opposite sign, and that this happens in only one direction (the up-down direction in Fig. 3). This is the property which leads to the names D and S for cells in which next-nearest neighbors are "dissimilar" and "similar." (References 30 and 34 refer to D and S cells as α and β clusters, respectively.)

Suppose that a D cell appears somewhere in the lattice. Rotate the lattice so that this D cell is oriented as in Fig. 3. Then all four of the conventional unit cells which overlap the original cell horizontally (such as the dotted cell in Fig. 3) must also be D cells because they contain next-nearest-neighbor spins of opposite sign. (These new cells will be oriented upside down relative to the original.) Consideration of the cells which overlap these cells horizontally, and the cells which overlap them, and so forth, demonstrates that the entire horizontal layer must be made up of D cells. It follows that all three of the horizontal (100) planes that intersect the origin cell are checkered.

On the other hand, suppose that there are no D cells in the lattice, i.e., that the lattice consists entirely of S and S' cells. Then an identical argument concerning an initial S (or S') cell and its horizontally overlapping cells implies that the lattice possesses three adjacent checkered (100) planes.

Now we show that if one (100) layer is checkered, then the layer two above (or below) it must also be checkered. Rotate the lattice so that the checkered plane is horizontal, and consider all the conventional unit cells which have

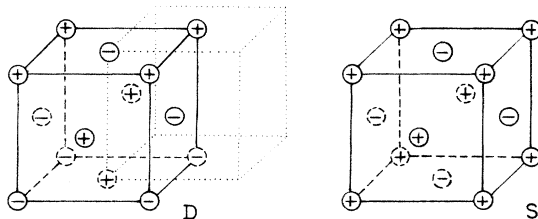


FIG. 3. Two conventional unit cells made up entirely of type-2 tetrahedra. A plus represents an up spin or A atom, a minus represents a down spin or B atom. Note that the appearance of these cells changes dramatically if they are set on their sides.

the given layer as their base. Because the base layer is checkered, these cells, whether D , S , or S' , must be oriented with the same vertical axis as the cells shown in Fig. 3. By the argument given above, either all or none of these cells are D cells. In either case, the layer formed by the tops of the unit cells, that is the layer two above the original layer, is again checkered.

Starting with the three layers already determined to be checkered and applying this result repeatedly, we conclude that all the (100) planes of any type-2 ground state must be checkered, as asserted above.

The verification of the type-3 ground-state description is even simpler. In this case there are three possible conventional unit cells (Fig. 4). It is quite easy to see that the four cells horizontally adjacent to (not overlapping) a given cell must be of the same type as the original cell, whence any configuration must have a down (100) layer sandwiched between two checkered layers. Finally, if a given layer is checkered then the adjacent layer is spin down and the layer two above is checkered, so the ground state must consist of alternating spin-down and checkered layers.

IV. LOW-TEMPERATURE STATES

One intuitively expects that a system's low-temperature states will qualitatively resemble its zero-temperature (i.e., ground) states. Thus the highly degenerate ground states of the fcc Ising antiferromagnet might lead one to expect highly disordered low-temperature states, in contrast to the usual low-temperature states in which a few defects are scattered about in the (single) ground state. This expectation is in fact quite incorrect. A Monte Carlo simulation of this model at low temperatures and with, say, $\alpha = \beta = \mu = 0$ (well into the regime of type-2 ground states) almost always finds the system in some small perturbation of a particular, highly symmetric ground state, the so-called " L_1 " (or " AB ") state (to be described later). In other words, the system behaves as if the infinite number of other ground states did *not* exist. Why is this one ground state singled out from so many as the basis for the low-temperature states? A heuristic argument points to the low-energy excitations of the ground states, as follows: At zero temperature the only factor relevant in determining the states is energy, so all ground states are equally likely. But at any finite temperature, no matter how small, entropy is a factor. The ground state with the largest number of low-energy excitations will correspond to the lowest-temperature state of highest entropy, so it will

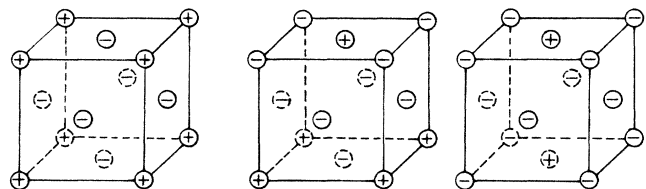


FIG. 4. The three conventional unit cells made up entirely of type-3 tetrahedra. Same notation as Fig. 3.

“dominate” the other ground states at low temperatures. (This argument was developed by Mackenzie and Young³⁴ and by Slawny,³⁵ who followed the work of Pirogov and Sinai;³⁶ see also Refs. 37 and 38. A precise version of the result was proved rigorously by Slawny and Bricmont.³⁹) In the case $\alpha=\beta=\mu=0$, the L_1 configuration is the dominant ground state (the one with the largest number of low-energy excitations), and this explains the Monte Carlo observation mentioned above.

In order to identify and describe the dominant ground states, we need a nomenclature which distinguishes among the many configurations which are type-1, -2, or -3 ground states. To this end, we call a (100) layer sandwiched between two checkered layers an “ S ” layer if the spins in the two adjacent layers point up in the *same* sublattice and a “ D ” layer if they point up in *opposite* sublattices. Notice that designation of a layer as D or S says nothing about the layer itself, which may be spin up, spin down, checkered, or otherwise, but instead says that the adjacent layers are checkered and are either “in phase” (similar, S) or “out of phase” (dissimilar, D). (It is true, however, that if a D layer is checkered then it consists entirely of D cells, and that if a S layer is checkered then it consists entirely of S and S' cells.)




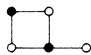

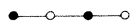
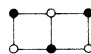
We show below that when $\alpha=\beta=0$, when $\alpha>0$, $\beta\leq 0$, and $\mu\leq 0$, or when $\alpha\leq 0$, $\beta>0$, and $\mu\geq 0$, then the dominant type-2 ground state consists entirely of S layers. This is the L_1 structure mentioned above. It is more easily visualized through either of the following

equivalent descriptions. (1) The L_1 structure consists of (100) layers which are alternatively spin up and spin down. (2) If the fcc lattice is dissected into its four interpenetrating simple-cubic sublattices, then in the L_1 structure two of the sublattices are occupied by up spins and two by down spins. We also show that when $\alpha=\beta=0$ and $\mu/v=4$, the dominant type-3 ground state is the L_2 configuration in which all the down layers are S layers. (Alternatively, one sublattice is occupied by up spins, three by down spins.) A similar result holds for the type-1 ground state when $\alpha=\beta=0$ and $\mu/v=-4$.

Clearly, vast volumes of the $(\alpha, \beta, \mu/v)$ parameter space are *not* treated in the above synopsis. We conjecture that the configurations given are in fact dominant throughout the relevant regions.

The remainder of this section is devoted to proofs of these assertions. Before starting, however, we must clarify the notion of a configuration with “the largest number of low-energy excitations.”³⁵ Consider the local excitations of a particular ground state. The energy increase caused by each excitation falls at some level on a discrete spectrum, and each energy level has a corresponding density of excitations. For example, the L_1 ground state at $\alpha=\beta=\mu=0$ has excitations of energy $4v$, $6v$, $8v$, $10v$, etc. Two types of excitations have energy $4v$: flipping a single up spin and flipping a single down spin. In a lattice of N sites there are $N/2$ ways to flip an up spin and $N/2$ ways to flip a down spin, so the total excitation density (excitations per lattice site) at this energy level is 1. Only one ex-

TABLE I. Important excitations of the type-2 ground state. The figures represent spins to be flipped in the excitation, with nearest-neighbor bonds indicated. An up spin (A atom) is indicated by a solid circle and a down spin (B atom) by an open circle. Thus one forms a type- B excitation by flipping an up spin and four adjacent down spins.

Excitation	Density	Energy
A 	$1 + n_S$	$8\epsilon'_1 + 8\epsilon'_3 = 8v - 12v\alpha - 12v\beta$
B 	$1 + n_S$	$24\epsilon'_1 = 12v - 36v\alpha + 6\mu$
B' 	$1 + n_S$	$24\epsilon'_3 = 12v - 36v\beta - 6\mu$
C 	$6 + 6n_S$	$14\epsilon'_1 + 6\epsilon'_3 = 10v - 21v\alpha - 9v\beta + 2\mu$
C' 	$6 + 6n_S$	$6\epsilon'_1 + 14\epsilon'_3 = 10v - 9v\alpha - 21v\beta - 2\mu$
E 	$96 - 4n_S$	$10\epsilon'_1 + 10\epsilon'_3$
F 	$2 + 2n_{SS}$	$10\epsilon'_1 + 10\epsilon'_3$

citation contributes at energy $6v$: it consists of flipping two adjacent spins of opposite sign, and it has density 4. To decide which of two ground states supports the “largest number of low-energy excitations” we compare the excitation density level by level, starting at the lowest excitation energy. If, at a given level, one ground state supports a greater density of excitations, then the ground state *dominates* the other and the comparison ceases. On the other hand, if the two ground states support an equal density of excitations at this level, the comparison goes to the next higher level and begins again. Note that the comparison hinges upon only the lowest level at which the two states differ. Thus if ground states X and Y have identical excitation densities up to the fifth level, and X dominates Y at the fifth level, then X dominates Y even if Y has many more excitations than X at the sixth level: excitations at the sixth and higher levels are called *irrelevant* in the determination of the dominant state. If one ground state dominates all others at a given point in the parameter space, then it is *dominant* in the sense described above and it forms the basis of the system’s unique low-temperature equilibrium state. If several ground states dominate all remaining ground states but not each other (as may happen because of symmetry), each will form a low-temperature equilibrium state and at the system will generally show phase coexistence among these states. (This procedure may fail when the ground-state degeneracy is too high: see Refs. 35–39.)

We begin our proofs by considering the type-2 ground state. We have cataloged all the excitations of the type-2 ground state with energy $10v$ or less at $\alpha=\beta=\mu=0$. Surprisingly few of these excitations (five out of 23) have densities dependent upon which type-2 ground state is being perturbed. These five excitations, along with two others of great importance, are described in Table I. The excitation energies in that table are given in terms of the variables

$$\epsilon'_1 \equiv \epsilon_1 - \epsilon_2 \quad \text{and} \quad \epsilon'_3 \equiv \epsilon_3 - \epsilon_2, \quad (9)$$

which are positive in the regime of type-2 ground states. The densities are given in terms of n_S , the fraction of (100) planes which are S layers, and n_{SS} , the fraction of adjacent pairs of layers which are both S layers. Excitation E is the only one which favors D over S layers in the dominant state, but excitations E and F are irrelevant for determining dominance, because their energy is always greater than that of excitation A . Excitation C is likewise irrelevant, because when the energy of B is lower than that of A then the energy of C is greater than the energy of B , whereas when the energy of A is lower than that of B then the energy of C is greater than the energy of A . Thus C is never the lowest-energy excitation with a density dependent on the ground state. Excitation C' can be proven irrelevant by similar reasoning. Although the remaining excitations A , B , and B' all favor the dominance of the $L 1_0$ configuration, there are an infinite number of other excitations that have not been examined. We prove that such excitations are irrelevant in three regions: first when $\alpha=\beta=0$ with μ arbitrary, then when $\alpha>0$, $\beta\leq 0$, and $\mu\leq 0$, and finally when $\alpha\leq 0$, $\beta>0$, and $\mu\geq 0$.

Let us take $\alpha=\beta=0$. The excitation energies of A , B ,

and B' are plotted in Fig. 5(a). Note (see Fig. 2) that the type-2 ground-state regime extends from $\mu/v=-2$ to $\mu/v=2$, so it terminates when the energy of a B (or B') excitation vanishes. By definition, in fact, the boundary of any ground-state regime is marked by the vanishing of some excitation energies, and *vice versa*: this is crucial to our arguments. The excitations that we must prove irrelevant fall into two classes: those with energy $12v$ at $\mu=0$, excluding B and B' , and those with energy greater than $12v$ at $\mu=0$. We have listed all 54 excitations of the first class, and they all have energies of $12v$, of $12v\pm 2\mu$, or of $12v\pm 4\mu$ [for example, the dashed line in Fig. 5(a)]. These energies are bounded below by the energy of either A , B , or B' , so such excitations are irrelevant. Now consider excitations of the second class. Because all excitation energies are linear in μ , and because they can only intersect the μ axis outside of the type-2 regime $-2 < \mu/v < 2$ [for example, the dotted line in Fig. 5(a)], such excitation energies are bounded below by the energy of B or B' . These excitations are again irrelevant, so at $\alpha=\beta=0$ the dominant type-2 ground state is $L 1_0$.

We turn to the case $\alpha>0$, $\beta\leq 0$. The excitation energies shift from those of Fig. 5(a) to those of Fig. 5(b), but the boundaries of the type-2 regime are still marked by the vanishing of the energies of B and B' at $\mu/v=-2+6\alpha$ and $\mu/v=2-6\beta$, respectively. Note that the energy versus μ line for a given excitation will change in intercept but not in slope. Thus to show that the uncataloged excitations are irrelevant when $\mu/v\leq 0$ we need only prove that their energies at $\mu=0$ cannot be less than that of B . Because any excitation energy is of the form

$$m_0\epsilon'_0 + m_1\epsilon'_1 + m_3\epsilon'_3 + m_4\epsilon'_4, \quad (10)$$

where the m_n are integers and where

$$\begin{aligned} \epsilon'_0 &\equiv \epsilon_0 - \epsilon_2 = 2v + \frac{1}{2}\mu, \\ \epsilon'_1 &\equiv \epsilon_1 - \epsilon_2 = \frac{1}{2}v - \frac{3}{2}v\alpha + \frac{1}{4}\mu, \\ \epsilon'_3 &\equiv \epsilon_3 - \epsilon_2 = \frac{1}{2}v - \frac{3}{2}v\beta - \frac{1}{4}\mu, \\ \epsilon'_4 &\equiv \epsilon_4 - \epsilon_2 = 2v - \frac{1}{2}\mu, \end{aligned} \quad (11)$$

we can rephrase our objective as follows: We wish to prove that if energy (10) exceeds or equals $24\epsilon'_1$ at

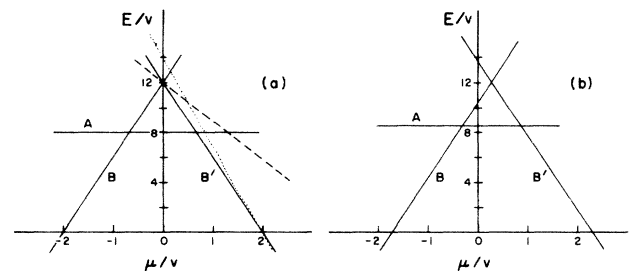


FIG. 5. Energies of the A , B , and B' excitations (see Table I) as a function of μ : (a) $\alpha=\beta=0$, (b) $\alpha>0$, $\beta<0$. The B' line slides rigidly to the right as β is decreased, and the B line slides rigidly to the right as α is increased.

$\alpha = \beta = \mu = 0$, then it continues to do so when $\alpha > 0$, $\beta \leq 0$, and $\mu = 0$. Or, in yet another form: If we denote the $\alpha = \beta = \mu = 0$ value of (10) by E_{000} , then we wish to prove that

$$E_{000} \geq 12v \quad (12)$$

implies

$$E_{000} - m_1(\frac{3}{2}v\alpha) - m_3(\frac{3}{2}v\beta) \geq 12v - 36v\alpha. \quad (13)$$

This result is obviously true if $m_3 > 24$, because then

$$m_0\epsilon'_0 + m_1\epsilon'_1 + m_3\epsilon'_3 + m_4\epsilon'_4 > 24\epsilon'_3, \quad (14)$$

which includes (13) as a special case, holds even without preconditions. On the other hand, if $m_3 \leq 24$, then we have

$$-m_3(\frac{3}{2}v\alpha) \geq -24(\frac{3}{2}v\alpha) \quad (15)$$

and, because $\beta \leq 0$,

$$-m_3(\frac{3}{2}v\beta) \geq 0. \quad (16)$$

Summing (12), (15), and (16) gives the desired result (13), so the proof is finished. A symmetrical argument proves that the L_1 configuration is also dominant when $\alpha \leq 0$, $\beta > 0$, and $\mu \geq 0$.

Our result for the dominant type-3 ground state is quite easy to prove, but only because it is so restricted—it involves only a single point in $(\alpha, \beta, \mu/v)$ space. We have cataloged the nine excitations with energies less than or equal to $8v$ when $\alpha = \beta = 0$ and $\mu/v = 4$, and have found that only one has a density dependent upon the ground state perturbed. This is excitation *A* of Table I, which has energy

$$8(\epsilon_4 - \epsilon_3) + 8(\epsilon_2 - \epsilon_3) = 8v(1 + 3\beta) \quad (17)$$

and density

$$1 + n_S, \quad (18)$$

where n_S is now the fraction of spin-down (100) layers which are *S* layers. [Recall that in a type-3 ground state, only half of the (100) layers, namely, the spin-down layers, can be described as *D* or *S*.] This proves the dominance of the L_2 configuration at $\alpha = \beta = 0$ and $\mu/v = 4$. The dominance of the L_2 type-1 ground-state configuration at $\alpha = \beta = 0$ and $\mu/v = -4$ follows from symmetry.

V. MONTE CARLO SIMULATIONS

In principle, the Pirogov-Sinai theory described in the preceding section can give a complete and rigorous description in the low-temperature phase diagram of our fcc Ising model away from the “superdegenerate” planes which bound each of the five different ground-state regimes in $(\alpha, \beta, \mu/v)$ space. We have, however, already seen that in practice the Pirogov-Sinai prescription may be too difficult to carry out. Furthermore, the most interesting features of the model are its phase transitions, which do not occur at “low” temperatures (except precisely near the superdegenerate points). To investigate the finite-temperature behavior of the system we turn to

Monte Carlo simulation. In doing so we pay two prices: First, we lose any semblance of rigor. Second, we can no longer keep α and β as free parameters, and it is prohibitively expensive to investigate more than a few points on the (α, β) plane. We have decided to investigate only one point on that plane, namely $\alpha = 0.01$, $\beta = -0.08$ (corresponding to $J_3/J_2 = 0.03375$, $J_4/J_2 = -0.0525$). Kikuchi and de Fontaine^{18,19} investigated the model with these parameters in the CVM approximation, and found that the resulting phase diagram was a reasonable likeness of the experimental phase diagram of copper-gold. This value of J_4 is perhaps too large to correspond to a realistic physical alloy,^{15,16} but the value of J_3 is certainly reasonable, and the interesting feature of the phase diagram, namely its asymmetry, is induced by J_3 alone.

We performed Monte Carlo simulations on an fcc lattice of 2408 sites (a cube with eight conventional unit cells on each edge), using single-spin-flip kinetics (Glauber dynamics). The computations were run on a CDC 7600 computer at Los Alamos National Laboratory and required less than one minute of CPU time per one million attempted spin flips. Experiments were begun with the system in a random configuration, then run for 2000 Monte Carlo steps per site to equilibrate and for 3000 Monte Carlo steps per site to collect data. To test the adequacy of this equilibration procedure we reran all our $\mu = 0$ simulations with an L_1 , rather than a random, initial state. The equilibrium energies measured in corresponding runs with different initial configurations differed by less than 4%, far less than the expected sampling errors. As expected, the acceptance ratio (i.e., the percentage of Monte Carlo steps accepted in the data taking portion of the simulation) was small at low temperatures and grew with temperature, with a large increase at the phase transition. For example, at $\mu = 0$ the acceptance ratio jumped from 11% to 21% at the transition.

Finite-size effects seem to be unimportant. For example, when the simulation at temperature $k_B T/v = 1.0$ and chemical potential $\mu = 0$ was performed on lattice portions of 256, 864, and 2048 sites (corresponding to cubes with four, six, and eight unit cells on an edge), the equilibrium energies per site were $e/v = -0.7 \pm 0.1$, -0.67 ± 0.03 , and 0.66 ± 0.01 , respectively. The transition temperatures determined from a sequence of simulations at different temperatures (as described below), are, for the three sizes, $k_B T_t/v = 1.00 \pm 0.05$, 0.98 ± 0.02 , and 0.967 ± 0.003 , respectively. In both cases increased size leads to increased accuracy, and does not drive the result out of the range established by smaller systems.

Fourteen values of the chemical potential were selected for detailed investigation, and for each chemical potential simulations were performed at 10 or 15 temperatures. A plot of equilibrium energy as a function of temperature for one of the chemical potentials, namely $\mu = 0$, is shown in Fig. 6. The error bars in this figure represent plus or minus one standard deviation (σ) among the energies sampled in more than six million data collecting Monte Carlo steps. This “sampling error” cannot be reduced to zero, because even in a simulation with an infinite number of Monte Carlo steps, it is related to the specific heat $c_\mu = (\partial e / \partial T)_\mu$ by the fluctuation-susceptibility relation

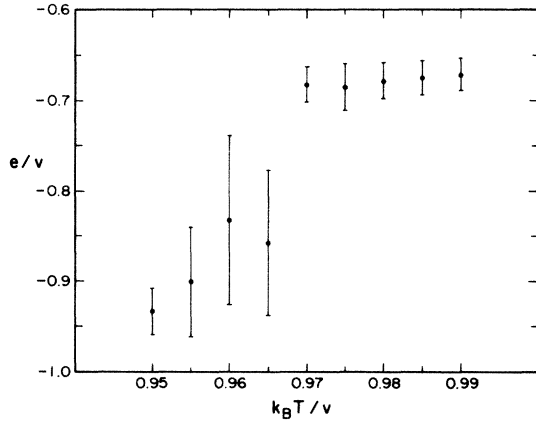


FIG. 6. Equilibrium energy as a function of temperature at fixed $\alpha=0.01$, $\beta=-0.08$, and $\mu=0.0$. The energies were determined by Monte Carlo simulation, and the error bars represent plus or minus one standard deviation among the energies sampled in the data taking portions of the simulations. From this graph we conclude that the transition is first order and that it falls between $k_B T/v=0.965$ and $k_B T/v=0.970$, as reported in Table II.

$$\sigma^2 = k_B T^2 c_\mu / N, \quad (19)$$

where N is the number of lattice sites in the simulation. A glance at Fig. 6 verifies qualitatively that this relation, which is obeyed exactly only by infinitely long simulations, is obeyed approximately in our work: the e versus T curve is steeper to the left, and the standard deviations are larger there. A quantitative examination confirms this conclusion, and increases our confidence that the simulations were carried out using an “effectively infinite” number of Monte Carlo steps.

The first-order phase transition was located by looking for approximate discontinuities in the energy as a function

TABLE II. Transition temperatures T_t and latent heats Δe , measured in units of the pair interaction v , at $\alpha=0.01$, $\beta=-0.08$, as determined by Monte Carlo simulation.

μ/v	$k_B T_t/v$	$\Delta e/v$
5.0	0.480 ± 0.005	0.06 ± 0.02
4.5	0.650 ± 0.005	0.12 ± 0.03
4.0	0.708 ± 0.003	0.13 ± 0.04
3.5	0.687 ± 0.003	0.07 ± 0.05
3.0	0.615 ± 0.005	0.02 ± 0.03
1.5	0.807 ± 0.003	0.10 ± 0.06
1.0	0.910 ± 0.005	0.19 ± 0.05
0.5	0.955 ± 0.005	0.23 ± 0.06
0.0	0.967 ± 0.003	0.17 ± 0.10
-0.5	0.913 ± 0.003	0.16 ± 0.07
-1.0	0.807 ± 0.003	0.06 ± 0.06
-3.5	0.930 ± 0.005	0.14 ± 0.06
-4.0	0.950 ± 0.005	0.12 ± 0.09
-4.5	0.918 ± 0.003	0.16 ± 0.06

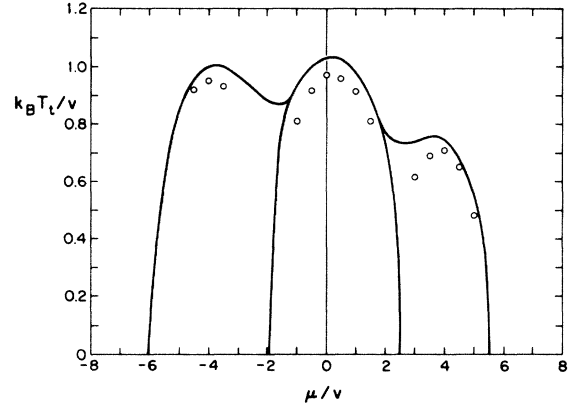


FIG. 7. Phase diagram (transition temperature as a function of chemical potential) for the model with $\alpha=0.01$, $\beta=-0.08$. The transition temperatures from CVM (Refs. 18, 20, and 40) are shown as a solid line, those from Monte Carlo as circles (the transition temperature error shown in Table II is smaller than the circles). The $T=0$ transition points are known exactly from the ground-state analysis: They are, from left to right, $\mu/v = -6-6\alpha$, $-2+6\alpha$, $2-6\beta$, and $6+6\beta$.

of temperature at fixed chemical potential (see Fig. 6). The transition temperatures and latent heats of transition, as surmised from the Monte Carlo experiments, are given in Table II. (The error in transition temperature is due to the finite-temperature steps between different simulations. The error in latent heat arises from sampling error in the energy at either side of the transition. As noted above, our equilibration times were long enough that the traditional difficulties with hysteresis and metastability near the first-order transition appear to be absent.) The Monte Carlo phase diagram is graphed and compared with the CVM results^{18,20,40} in Fig. 7. Note the paucity of Monte Carlo results at low temperatures. This is because the latent heat becomes small at low temperatures, and the transition is lost when the latent heat shrinks to the size of the Monte Carlo sampling errors. (Thus we cannot clarify the question of whether the L_{10} , L_{12} triple points fall at finite or zero temperature.^{5,8} We do point out, however, that this question, which has been investigated in the nearest-neighbor case, remains even when α and β do not vanish.) By using more elaborate techniques Monte Carlo can in fact track such low latent heat transitions,⁸ but we have decided to focus instead on the most dramatic feature of the phase diagram, namely its asymmetry.

The Monte Carlo phase diagrams with and without multiatomic interactions are shown in Fig. 8. It is remarkable that such a small value of J_3 , barely more than 3% of J_1 , can depress the right-hand local maximum by about 25%. In addition, the multiatom interaction raises the central and left-hand maxima in such a way that the central maximum, which is the lowest of the three when $\alpha=\beta=0$, becomes the highest. Note also that the temperatures of the maxima shift much more than their chemical potentials do, although the central maximum is displaced visibly to the right from $\mu=0$.

It would be interesting to follow the change in latent

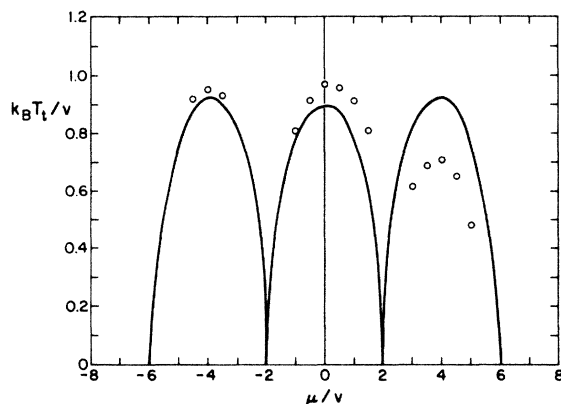


FIG. 8. Phase diagram of the model with and without multiatomic interactions. The circles are the Monte Carlo transitions when $\alpha=0.01$, $\beta=-0.08$ (as in Fig. 7); the line is the transition observed when $\alpha=\beta=0$ in the Monte Carlo work of Binder (Ref. 8).

heats of transition upon the addition of multiatomic forces, as we have just followed the change in the phase diagram, but the relevant latent heats at $\alpha=\beta=0$ are not available. The only comparison currently possible is at $\mu=0$, where the $\alpha=\beta=0$ latent heat is $\Delta e/v=0.17$,⁶ identical to the value at $\alpha=0.01$, $\beta=-0.08$ (see Table II). Whether this agreement is significant or a coincidence cannot be decided until more latent heats at several values of α , β , and μ become available.

Finally, we comment upon the reliability of the cluster-variation method in this problem. Figure 7 shows that the CVM seems to always overestimate the transition temperature, as is expected of a mean-field-like theory. The same overestimate appears in the nearest-neighbor case,^{5,8} and in fact, the CVM seems to give transition tem-

peratures which are so consistently high that they accurately mirror the phase diagram distortions induced by the multiatom forces. Thus at $\alpha=\beta=\mu=0$ the transition temperatures $k_B T_t/v$ predicted by CVM (tetrahedron approximation)² and by Monte Carlo (MC) methods⁶ are 0.947 and 0.883, respectively, so CVM exceeds MC by 7.2%. At $\alpha=0.01$, $\beta=-0.08$, $\mu=0$ the CVM (Ref. 40) and MC transitions are 1.026 and 0.967, so the CVM excess is 6.0%. In contrast to this near-agreement near stoichiometry, the CVM and MC results diverge markedly near the superdegenerate points (i.e., the boundary points between different ground states). This feature has already been noticed in the nearest-neighbor case,⁸ but it may be due as much to inadequacies in the Monte Carlo method, which has known difficulties at low temperatures, as to inadequacies in the CVM.

Note added in proof. After submitting this article, we found that J. M. Bell⁴¹ has investigated the problem using a closed-form approximation technique.

ACKNOWLEDGMENTS

We thank the Center of Materials Science at Los Alamos National Laboratory for providing the computer time which made the Monte Carlo simulations possible, and are grateful for the assistance and hospitality of Dr. James Gubernatis in carrying out this phase of the work. Joseph Slawny, Jean Bricmont, and Ryo Kikuchi graciously informed us of their unpublished research results. We gratefully acknowledge useful discussions with these scientists and also with Juan Sanchez and John Cahn. This work has enjoyed the support of the U.S. Air Force Office of Scientific Research through Grant No. 85-0014.

*Present address: Department of Physics, Oberlin College, Oberlin, OH 44074.

†Permanent address: Department of Physics, Indian Institute of Science, Bangalore 560 012, Mysore, India.

¹C. Domb, in *Phase Transitions and Critical Phenomena*, edited by C. Domb and M. S. Green (Academic, London, 1974), Vol. 3, pp. 357–483.

²C. M. van Baal, *Physica (Utrecht)* **64**, 571 (1973).

³R. Kikuchi and H. Sato, *Acta Metall.* **22**, 1099 (1974).

⁴N. S. Golosav, L. E. Popov, and L. Ya. Pudan, *J. Phys. Chem. Solids* **34**, 1149 (1973); **34**, 1157 (1973).

⁵J. M. Sanchez, D. de Fontaine, W. Teitler, *Phys. Rev. B* **26**, 1465 (1982).

⁶M. K. Phani, J. L. Lebowitz, M. H. Kalos, and C. C. Tsai, *Phys. Rev. Lett.* **42**, 577 (1979).

⁷M. K. Phani, J. L. Lebowitz, and M. H. Kalos, *Phys. Rev. B* **21**, 4027 (1980).

⁸K. Binder, *Phys. Rev. Lett.* **45**, 811 (1980).

⁹K. Binder, J. L. Lebowitz, M. K. Phani, and M. H. Kalos, *Acta Metall.* **29**, 1655 (1981).

¹⁰K. Binder, W. Kinzel, and W. Selke, *J. Magn. Magn. Mater.* **31-34**, 1445 (1983).

¹¹J. L. Lebowitz, M. K. Phani, and D. F. Styer, *J. Stat. Phys.* **38**, 413 (1985).

¹²J. M. Sanchez and D. de Fontaine, *Phys. Rev. B* **21**, 216 (1980).

¹³J. M. Sanchez and D. de Fontaine, *Phys. Rev. B* **25**, 1759 (1982).

¹⁴T. Mohri, J. M. Sanchez, and D. de Fontaine, *Acta Metall.* **33**, 1171 (1985).

¹⁵A. Bieber and F. Gautier, *J. Phys. Soc. Jpn.* **53**, 2061 (1984).

¹⁶A. Bieber and F. Gautier, *Z. Phys. B* **57**, 335 (1984).

¹⁷R. C. Kittler and L. M. Falicov, *Phys. Rev. B* **18**, 2506 (1978); **19**, 291 (1979).

¹⁸R. Kikuchi and D. de Fontaine, in *Applications of Phase Diagrams in Metallurgy and Ceramics*, Natl. Bur. Stand. (U.S.) Spec. Publ. No. 496 (U.S. GPO, Washington, D.C., 1978), Vol. 2, pp. 967–998.

¹⁹D. de Fontaine and R. Kikuchi, in *Applications of Phase Diagrams in Metallurgy and Ceramics*, Natl. Bur. Stand. (U.S.) Spec. Publ. No. 496 (U.S. GPO, Washington, D.C., 1978), Vol. 2, pp. 999–1026.

²⁰J. W. Cahn and R. Kikuchi, *Acta Metall.* **27**, 1329 (1979).

²¹R. Kikuchi and J. W. Cahn, *Acta Metall.* **27**, 1337 (1979).

²²R. Kikuchi, J. M. Sanchez, D. de Fontaine, and H. Yamauchi, *Acta Metall.* **28**, 651 (1980).

²³R. A. Bond and D. K. Ross, *J. Phys. F* **12**, 597 (1982).

²⁴M. Grimsditch, P. Loubeyre, and A. Polian, *Phys. Rev. B* **33**,

- 7192 (1986).
- ²⁵M. Roger, J. H. Hetherington, and J. M. Delrieu, *Rev. Mod. Phys.* **55**, 1 (1983).
- ²⁶K. G. Wilson, *Phys. Rev. D* **10**, 2445 (1974).
- ²⁷J. Kogut and L. Susskind, *Phys. Rev. D* **11**, 395 (1975).
- ²⁸P. W. Anderson, *Phys. Rev.* **79**, 705 (1950).
- ²⁹J. M. Luttinger, *Phys. Rev.* **81**, 1015 (1951).
- ³⁰A. Danielian, *Phys. Rev. Lett.* **6**, 670 (1961).
- ³¹O. J. Heilmann, *J. Phys. A* **13**, 1803 (1980).
- ³²O. G. Mouritsen, B. Frank, and D. Mukamel, *Phys. Rev. B* **27**, 3018 (1983).
- ³³D. Hajduković and S. Milošević, *J. Phys. A* **15**, 3561 (1982).
- ³⁴N. D. Mackenzie and A. P. Young, *J. Phys. A* **14**, 3927 (1981).
- ³⁵J. Slawny, *J. Stat. Phys.* **20**, 711 (1979).
- ³⁶S. A. Pirogov and Ya. G. Sinai, *Teor. Mat. Fiz.* **25**, 358 (1975); **26**, 61 (1976).
- ³⁷J. Slawny, in *Phase Transitions and Critical Phenomena*, edited by C. Domb and J. L. Lebowitz (Academic, London, 1985), Vol. 10.
- ³⁸Ya. G. Sinai, *Theory of Phase Transitions: Rigorous Results* (Pergamon, Oxford, 1982).
- ³⁹J. Slawny and J. Bricmont (unpublished); see also, E. I. Dinaburg and Ya. G. Sinai, *Commun. Math. Phys.* **98**, 119 (1985).
- ⁴⁰R. Kikuchi (private communication).